Available online at www.sciencedirect.com
SCIENCE DIRECT®
Catalysis Today 85 (2003) 321–331
CATALYSIS TODAY
www.elsevier.com/locate/cattod

Adsorption and reaction of acrolein on titanium oxide single crystal surfaces: coupling versus condensation

A.B. Sherrill [a], H. Idriss [a,1], M.A. Barteau [a,*], J.G. Chen [b]

[a] *Department of Chemical Engineering, Center for Catalytic Science and Technology, University of Delaware, Newark, DE 19716, USA*
[b] *Department of Materials Science and Engineering, Center for Catalytic Science and Technology, University of Delaware, Newark, DE 19716, USA*

Received 3 April 2003; received in revised form 17 April 2003; accepted 21 May 2003

Abstract

The reactions of acrolein have been investigated on TiO_2(0 0 1) single crystal surfaces by temperature programmed desorption (TPD), X-ray photoelectron spectroscopy (XPS) and near edge X-ray absorption fine structure (NEXAFS). Two carbon–carbon bond-forming reactions were observed. The first, on defect-containing surfaces, is reductive coupling to form olefins. The high reaction yield of ca. 80% shows the high activity of such surfaces for carbon–oxygen bond dissociation (needed for surface oxygen restoration) and carbon–carbon bond formation to make olefins. The second reaction, observed on the stoichiometric surface, is condensation of two acrolein molecules to give a C_6H_8O product tentatively identified as 2-methyl-2,4-pentadienal. Condensation reactions of carbonyls are characteristic of TiO_2 surfaces; for acrolein, this reaction is proposed to involve initial hydrogen addition followed by nucleophilic attack on a second molecule of acrolein. This results in an aldol condensation followed by dehydration.

NEXAFS analyses were conducted in order to differentiate the states of molecularly adsorbed acrolein on the two distinctly different surfaces. The C=O bond of adsorbed acrolein is maintained in the case of the stoichiometric surface (evidenced by a $\pi^*_{C=O}$ transition at 286.6 eV), while it is absent on the reduced surface. The absence of this NEXAFS transition on the reduced surface suggests that the O atom of the C=O bond has reacted with the oxygen-deficient lattice. The restoration of these oxygen deficiencies is concomitant with the formation of the reductive coupling products (as observed by TPD and XPS experiments).

Keywords: TiO_2(0 0 1) single crystal; Aldol condensation; Michael addition; NEXAFS-acrolein; Reductive-coupling

1. Introduction

The chemistry of oxygenates and hydrocarbons on the surfaces of transition metal oxides are relevant to a variety of catalytic processes, including selective oxidations and reductions. Of particular importance is the relationship between the structures of surface sites, both geometric and electronic, and surface intermediates. The struggle to obtain high reaction yields often requires finding new chemical pathways that may provide more efficient syntheses. This goal motivates attempts to improve our understanding of heterogeneous reaction processes. Surface science provides important tools for such investigations. Numerous

* Corresponding author. Tel.: +1-302-831-8905; fax: +1-302-831-8201.
E-mail address: barteau@che.udel.edu (M.A. Barteau).
[1] Present address: Department of Chemistry, The University of Auckland, Private Bag 92019, Auckland, New Zealand.

0920-5861/$ – see front matter © 2003 Elsevier B.V. All rights reserved.
doi:10.1016/S0920-5861(03)00398-5

catalytic reactions are carried out on transition metal oxides; these processes include hydrocarbon oxidation [1–3], syngas conversion [4–7], and dehydration reactions [8,9]. Titanium dioxide is a versatile oxide material in catalysis. Considerable number of chemical reactions catalyzed by TiO_2 alone or together with other oxides or metals are found. These include condensation reactions (TiO_2) [10,11], maleic and phthalic anhydride formation from butane and *o*-xylene, respectively (TiO_2/V_2O_5) [1–3], water-splitting to produce H_2 and O_2 (TiO_2, $SrTiO_3$, $Ni–K_2La_2Ti_3O_{10}$, and Pt/TiO_2) [12–14] for energy conversion, and photo-oxidation of organic molecules to form CO_2 (TiO_2) [15–19] for water and air decontamination. Previously, the chemical reactions of saturated and aromatic carbonyl compounds have been investigated on the surfaces of $TiO_2(0\,0\,1)$ single crystals. For reactants such as acetaldehyde that contain α-CH bonds, two carbon–carbon bond-forming reactions have been observed in ultra-high vacuum. The first is aldol condensation of two acetaldehyde molecules to form crotonaldehyde (an α,β-unsaturated C_4 aldehyde) [10]. The second is the reductive coupling of aldehydes to form symmetric olefins [20–25]. These reactions were observed in parallel work on TiO_2 powders at atmospheric pressure [26]. The condensation reaction was essentially observed on stoichiometric TiO_2 surfaces while reductive coupling was observed exclusively on titanium suboxide-containing surfaces. Base-catalyzed aldol condensation of aliphatic carbonyl compounds requires hydrogen abstraction from the α-carbon of the carbonyl and is thus effectively achieved by basic sites on the surface. This role is filled by the lattice oxygen of stoichiometric surfaces acting as Lewis base sites. Reductive coupling requires carbon–oxygen bond dissociation. The surfaces of titanium suboxides act as an oxygen sink, i.e., the driving force for this reaction is the filling of surface oxygen vacancies. This chemistry is fairly aggressive. For example, we have observed that more than 50% of the surface oxygen could be replenished by oxygen provided from the carbon–oxygen bond dissociation in the reductive coupling reactions of benzaldehyde [24] and *p*-benzoquinone [23] on reduced titania surfaces.

Acrolein is the simplest unsaturated aldehyde and is currently used for the production of D,L-methionine (an essential amino acid used as an animal feed supplement) [27]. It is also used for the production of other compounds such as acrylic acid [28], pyrans, and methylpyridine [29]. Several issues prompted this investigation of acrolein on TiO_2 single crystal surfaces. First, the conjugated character ($CH_2{=}CH–CH{=}O \leftrightarrow {}^{(+)}CH_2–CH{=}CHO^{(-)}$) of this α,β-unsaturated compound makes it a potentially useful probe of the extent to which electron delocalization affects carbon–oxygen bond dissociation as well as carbon–carbon bond formation on oxide surfaces. Second, one needs to know which function of the molecule—the olefin or the carbonyl group—will dominate the reaction. Experiments with acrylic acid indicated that the carboxyl group dominates its reactions on the stoichiometric surface, i.e., the reaction of the olefin function was negligible on the surfaces of TiO_2 single crystals [9], while the olefin group had substantial reactivity on the reduced surface [30]. Third, it has been observed in the case of formaldehyde [31] as well as of acetaldehyde [10] that oxidation reactions to form carboxylates are insignificant on the surfaces of TiO_2 single crystals in UHV. This is unlike other oxides such as ZnO [32,33] and CeO_2 [34] (more reducible materials) both of which can easily donate lattice oxygen to aldehydes in order to form carboxylates. Another important reason for studying this bifunctional molecule is to investigate condensation reactions on a well-defined surface. Condensation of carbonyls to α,β-unsaturated higher carbonyls is well known and was previously observed on the surface of TiO_2 single crystals. Acrolein cannot undergo this type of condensation (β-aldolization) directly, because of the strong vinylic C–H bond. However, we do see evidence for products of carbon–carbon bond formation reactions between acrolein molecules on TiO_2 surfaces, and potential mechanisms are presented and discussed here.

$TiO_2(0\,0\,1)$ single crystal surfaces have been studied in detail by X-ray photoelectron spectroscopy (XPS) [20–25,35,36], AES, LEED [8], UPS [36], and more recently by near edge X-ray absorption fine structure (NEXAFS) [37]. Ion-sputtered (reduced) surfaces contain titanium suboxides, the relative population of which can be altered by annealing in UHV at different temperatures [35]. Stoichiometric surfaces can be prepared by annealing at 750 K [8] and higher.

This work presents the reactions of acrolein by TPD, XPS and NEXAFS on the surfaces of a $TiO_2(0\,0\,1)$

single crystal and compares the reaction pathways to those of other carbonyl compounds previously examined.

2. Experimental

TPD experiments were conducted in a differentially pumped vacuum chamber (VG Mark II ESCALAB) with a base pressure of ca. 6×10^{-11} mbar. The chamber is equipped with a single-channel hemispherical analyzer, titanium sublimation pump, two-grid LEED optics, and a Hiden RCAPIC3 quadrupole mass spectrometer. A computer was used to multiplex the mass spectrometer. The heating rate of the sample was controlled at 1 K/s by a PID controller (Omega Engineering). Up to 20 masses were monitored at an interval of 2–3 s for the complete cycle. The TiO_2(0 0 1) single crystal (Commercial Crystal Laboratories) was mounted and cleaned by successive sputtering with argon ions and heating to 800 K for 60 min. Surface sputtering was carried out using a 2 keV beam (current = 25 mA) for 60 min at a base pressure of 3.5–5 $\times$ 10^{-7} mbar. The crystal was then flashed to 600 K to remove a portion of the implanted ions. Parallel XPS analysis indicated that no noticeable surface oxidation occurred during this procedure [35–38]. All TPD measurements were conducted on surfaces saturated with acrolein (produced by direct dosing of the surface at a background pressure of 3.5×10^{-9} mbar at 120 K, for ≈2 min). Acrolein was introduced into the chamber in a separate experiment in order to determine its mass spectrometer fragmentation pattern and sensitivity correction factor. The major fragments and their corresponding relative intensities (in parentheses) were as follows: *m*/*e* 56 (0.32), *m*/*e* 55 (0.26), *m*/*e* 29 (0.49), *m*/*e* 27 (1.0), and *m*/*e* 26 (0.58). The sensitivity factor for acrolein relative to CO, calculated following the method of Madix and co-workers [39], was equal to 7 for *m*/*e* 56. The fragmentation patterns of the following products were taken from mass spectrometry data in the literature [40], and the calculated correction factors are listed: propene (*m*/*e* 42: 5.3), allyl alcohol (*m*/*e* 31: 5.7), and 2-methyl-2,4-pentadienal (*m*/*e* 96: 30.6). The fragmentation patterns for the following products were taken from separate experiments performed on our UHV system, and the calculated correction factors are listed: 2,4-hexadiene (*m*/*e* 82: 21.1), 1,3,5-hexatriene (*m*/*e* 80: 9.9) and benzene (*m*/*e* 78: 2.9).

The NEXAFS measurements were conducted on the U1 beamline of the National Synchrotron Light Source (NSLS) at Brookhaven National Laboratory. The two-stage UHV chamber is equipped with an ion sputtering gun, a quadrupole mass spectrometer, and an Auger electron spectrometer. All NEXAFS spectra were recorded with a partial electron yield detector with a retarding voltage of −200 eV. The resolution of the synchrotron monochromator was set at 0.4 eV near the carbon K-edge region. All NEXAFS spectra reported have been divided by the signals from a reference grid, which measures the incident beam intensity simultaneously with the NEXAFS spectrum, and then by the corresponding ratio of the spectrum of a clean surface taken at the same incidence angle.

Quantum chemical computations for the adsorption of acrolein were conducted by the semi-empirical PM3 method provided by the Spartan 02 windows program (Wavefunction Inc.). A $Ti_8O_{29}H_{26}$ cluster was generated with Cerius 2 molecular simulation software and imported to Spartan (following the same procedure as in [41,42]). The cluster was frozen except for the central surface Ti atom labeled, and the adsorbed molecule was allowed to move freely.

The adsorption energy, E_{ads}, was computed as follows:

$$E_{ads} = E_{model} - (E_{bare} + E_{molecule})$$

where E_{model} is the energy of the adsorption complex, E_{bare} the energy of bare cluster, and $E_{molecule}$ the energy (heat of formation) of gas phase acrolein.

3. Results

Temperature programmed desorption (TPD) of acrolein has been studied on two different characteristic surfaces of a TiO_2(0 0 1)-oriented single crystal. The reduced surface prepared by Ar-ion sputtering contains Ti suboxides (in addition to Ti^{4+} cations) and the fully stoichiometric surface contains only Ti^{4+} cations [43]. The structure and reactivity of both surfaces have been extensively studied in other works [8–10,20–26,35–38,44]. Fig. 1 shows the main products resulting from acrolein TPD on the reduced (sputtered) TiO_2(0 0 1) single crystal surface (Table 1

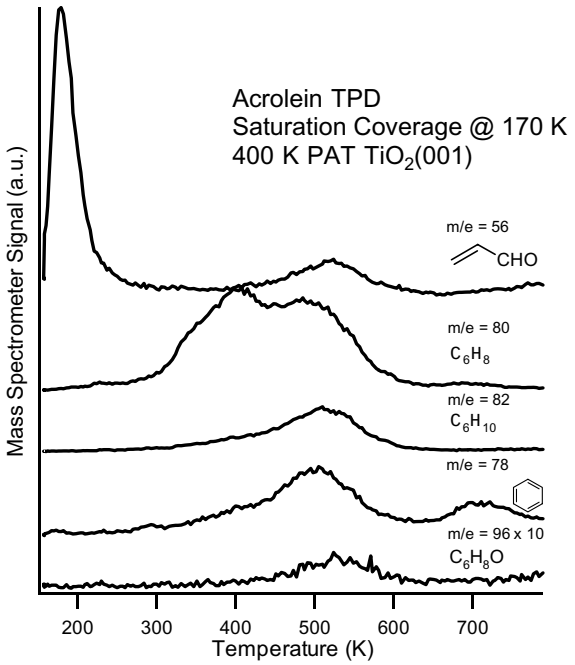

Fig. 1. TPD spectra of acrolein adsorbed on sputtered TiO_2(0 0 1) at 170 K: the desorption spectra of acrolein (*m*/*e* 56), hexatriene (*m*/*e* 80), hexadiene (*m*/*e* 82), benzene (*m*/*e* 78) and the C_6H_8O condensation product (*m*/*e* 96) are illustrated.

shows the quantitative analyses). Products were observed in three temperature domains. The first, at 200 K, represented desorption of adsorbed acrolein (*m*/*e* 56 in Fig. 1); the onset of desorption coincided with the start of the linear heating ramp. A second product desorption channel was observed between 380 and 410 K, which was largely composed of the reductive coupling product hexatriene (*m*/*e* 80).

Table 1
Relative product yield (%) from acrolein-TPD on reduced and stoichiometric TiO_2(0 0 1) single crystal surfaces[a]

Product	Temperature (K)	Reduced surface	Stoichiometric surface
Benzene	500, 700	2.5%	0.4%
Hexatriene	380–410, 500	49.8	4.7
Hexadiene	500	30.3	1.3
C_6H_8O	350–500	2.0	4.4
Allyl alcohol	380–410	1.2	0.3
Propene	380–410	14.2	0.5

[a] All percentages are expressed in terms of the total carbon content of products desorbing in experiments on the reduced surface.

Hexatriene formation by this pathway is in accord with previously observed reductive coupling reactions of aldehydes and ketones on reduced TiO_2(0 0 1) surfaces [20–25,35,36]. The sputtered surface contains hydrogen implanted during ion-bombardment and gettered during exposure of reactive, low-valent titanium cations to the UHV background after surface reduction. This results in partial hydrogenation of adsorbed organics [45]. In the present case hexadiene (*m*/*e* 82), derived from the partial hydrogenation of hexatriene, desorbed at 500 K, coincident with a second desorption channel for hexatriene. Benzene (*m*/*e* 78) also desorbed at this temperature, a likely product of dehydrocyclization of hexatriene. A small amount of the oxygen-containing product C_6H_8O (*m*/*e* 96) also desorbed at a 2% yield. The *m*/*e* 96 desorption product was coincident with signals from *m*/*e* 65, 67, and 95 and is attributed to 2-methyl-2,4-pentadienal. The ratio of *m*/*e* 96 to *m*/*e* 67 is 0.26. Both 2,4-dimethylfuran and 1-formyl cyclopentene (each having a C_6H_8O stoichiometry) are also known to give rise to large signals for *m*/*e* 65, 67, 95, and 96 [40], and are potential candidates to explain this product. However, since a route to 2-methyl-2,4-pentadienal can be sketched with minimal involvement of steps not previously documented on TiO_2 surfaces, the *m*/*e* 96 peak in Fig. 1 is thus attributed to that product (see Section 4). A still higher temperature desorption feature for benzene at 700 K is likely due to cyclotrimerization of surface acetylides at Ti^{2+} sites; formation of benzene from surface acetylides has previously been demonstrated in studies of acetylene chemistry on the sputtered TiO_2(0 0 1) surface [46].

Fig. 2 and Table 1 present the products observed in acrolein TPD on a TiO_2(0 0 1) surface annealed to 900 K for 45 min. This surface is fully oxidized and contains no Ti suboxides within the sensitivity of XPS [8,24,38], UPS [36], and NEXAFS [47]. Important reactivity changes occurred upon annealing. The total carbon capacity of the surface was only about 15% of the capacity of the sputtered surface as determined by XPS. This is simply due to re-crystallization of the amorphous surface produced by Ar-ion bombardment. Acrolein desorbed from the oxidized surface in two peaks. The first, at 200 K, is the desorption of molecular acrolein, likely from a condensed state, while the second occurs from a more stable molecularly adsorbed state at 280 K. The yield of coupling products

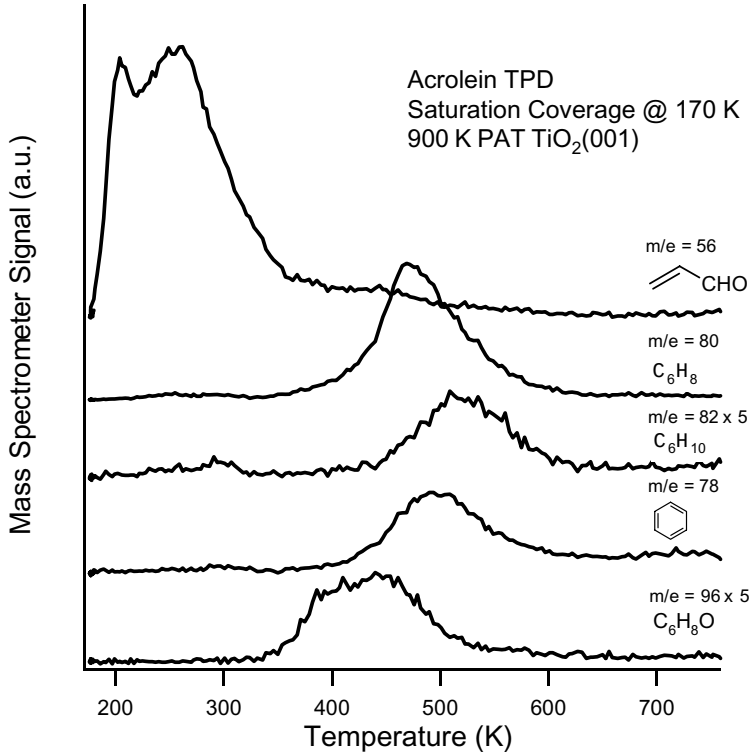

Fig. 2. Acrolein TPD performed on the 900 K-annealed surface, representing the stoichiometric TiO_2(0 0 1) surface.

declined considerably, dropping from almost 80% on the sputtered surface to 6.4% on the 900 K-annealed surface. Hexatriene, hexadiene, and benzene desorbed nearly simultaneously at 500 K. There was no lower temperature state for hexatriene. The existence of the reductive coupling reaction at all on the stoichiometric surface suggests that acrolein may be utilized to find point oxygen vacancies below the level detectable by spectroscopic methods. The production of the condensation product C_6H_8O doubled on the 900 K-annealed surface, although it was still outpaced by the production of coupling products. The condensation product also shifted down in temperature, developing as a broad feature desorbing from the surface between 350 and 500 K.

NEXAFS measurements of acrolein-derived adlayers on both the sputtered (reduced) and 900 K-annealed (stoichiometric) surfaces of TiO_2(0 0 1) were carried out. Acrolein was adsorbed on the surface as in a normal TPD experiment, and the crystal was heated at 1 K/s to 250 K to desorb multilayer acrolein; the NEXAFS spectrum was then recorded. After NEXAFS data collection, the crystal was heated to 350 K (400 K in the case of the reduced surface) and a second NEXAFS spectrum was collected.

Fig. 3 illustrates the normal incidence NEXAFS spectra for acrolein adsorbed on the 900 K-annealed surface. A NEXAFS transition at 285.4 eV is assigned as the $\pi^*_{C=C}$ feature corresponding to the vinyl group of the acrolein molecule. A transition at 286.6 eV is present, and is characteristic of a $\pi^*_{C=O}$ anti-bonding orbital (as was also observed for benzaldehyde on TiO_2(0 0 1) [48]). Consequently, the spectrum at 250 K is characteristic of chemisorbed acrolein on this oxidized surface. The NEXAFS transitions at 289.4 and 293.0 eV are characteristic of σ^*_{C-H} and σ^*_{C-C} features, respectively. Upon heating to 350 K, the edge-jump is further reduced, consistent with desorption from the surface. While the low carbon coverage makes analysis of the 350 K spectrum difficult, it is apparent that the $\pi^*_{C=O}$ feature at 286.6 eV has disappeared from the spectrum. The $\pi^*_{C=C}$ fea-

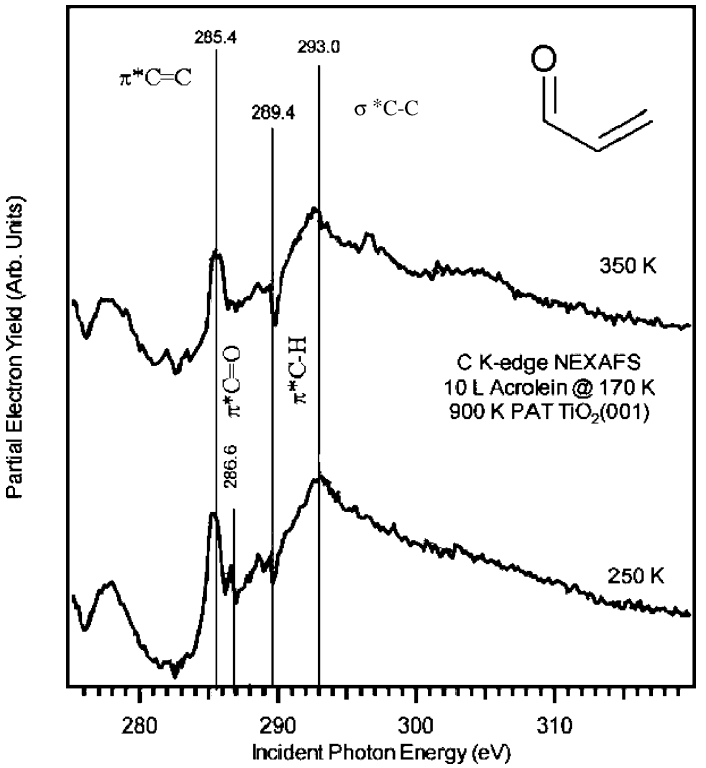

Fig. 3. Carbon K-edge NEXAFS for acrolein adsorbed on {1 1 4}-faceted TiO_2(0 0 1) at 170 K. The lower spectrum was recorded after heating to 250 K; the upper spectrum was recorded after heating to 350 K.

ture at 285.2 eV decreases in intensity; there is no apparent change in the intensity of the $\sigma^*_{C–H}$ and $\sigma^*_{C–C}$ features.

Fig. 4 illustrates the NEXAFS spectra for the acrolein-dosed reduced surface of TiO_2(0 0 1). The presence of the narrow and intense $\pi^*_{C=C}$ feature at 285.4 eV indicates that the vinyl groups of the acrolein molecules are unperturbed by the surface, and thus are likely positioned away from the surface. The absence of a $\pi^*_{C=O}$ feature at 286.6 eV, unlike in the case of the 900 K-annealed surface, suggests that the oxygen atom in the carbonyl group is no longer sp^2-hybridized, most likely due to its insertion into the lattice vacancy. Thus, this NEXAFS spectrum is consistent with an intermediate structure comparable to the pinacolate intermediate proposed for reductive carbonyl coupling reactions on TiO_2(0 0 1) [24]. The NEXAFS spectrum at 250 K also shows the characteristic $\sigma^*_{C–H}$ and $\sigma^*_{C–C}$ features at 289.0 and 292.6 eV, respectively.

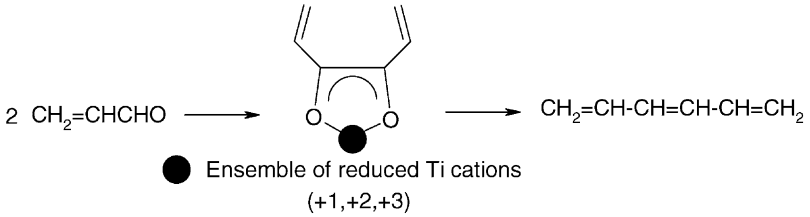

The 400 K NEXAFS spectra reveal a change in adsorbate bonding. Hexatriene and hexadiene start to desorb from the reduced TiO_2(0 0 1) surface in this temperature region; the NEXAFS tran-

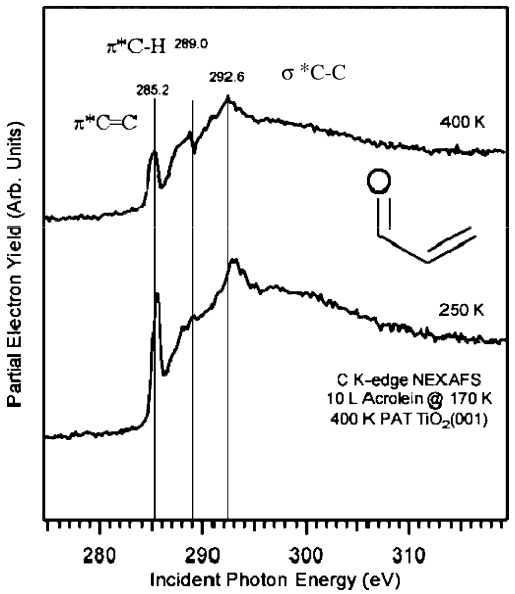

Fig. 4. Carbon K-edge NEXAFS for acrolein adsorbed on sputtered $TiO_2(0\,0\,1)$ at 170 K. The lower spectrum was recorded after heating to 250 K; the upper spectrum was recorded after heating to 400 K.

sition at 285.2 eV is broadened and attenuated relative to that at 250 K, indicative of interaction of the $\pi^*_{C=C}$ orbitals with the crystal surface after heating to 400 K. Scheme 1 shows a possible intermediate in the reductive coupling of acrolein.

The pinacolate, proposed here, has been proposed before for identical reactions of benzaldehyde [24], as well as for reductive coupling reactions carried out in slurries containing low-valent metal cations [19]. The NEXAFS spectrum for the 250 K surface suggests that the vinyl groups in Scheme 1 were lifted away from the surface. After heating the surface to 400 K, the NEXAFS spectrum suggests that the vinyl groups rotated down, as they might with flat-lying hexatriene or hexadiene. The NEXAFS σ^*_{C-H} (289.0 eV) and σ^*_{C-C} (292.6 eV) transitions have not shifted outside of the resolution of the spectrometer (0.4 eV) with respect to the 250 K spectrum. The NEXAFS edge-jump has diminished somewhat, consistent with desorption of carbon-containing species from the surface of the crystal.

4. Discussion

4.1. Olefins versus carbonyls on TiO_2 single crystal surfaces

The data from acrolein TPD and NEXAFS on the reduced surfaces of TiO_2 clearly indicated the absence of a direct interaction between the olefin group (CH_2=CH–) and the surface. This is in contrast to the reactions of the corresponding acid (acrylic acid) [30]. Previous work indicated that de-carboxylation of acrylic acid is favored on the reduced surface, giving CO_2 and a hydrocarbon fragment (that undergoes coupling subsequently). On the other hand, de-carbonylation of the aldehyde is not favored; the dominant reaction is reductive coupling (see Section 4.2). Interaction of acrolein with the surface via both the carbonyl and olefin functions would likely result in propionaldehyde formation due to facile hydrogenation of the vinyl group. Propionaldehyde was not observed during TPD, however. Thus the intra-molecular competition for surface sites is far more in favor of the C=O function rather than the CH_2=CH– function. In order to obtain some insight into the strength of the interaction of both functional groups of acrolein with the surface, we have conducted PM3 calculations on a $Ti_8O_{29}H_{26}$ charge-neutral cluster representing the $TiO_2(0\,1\,1)$ surface. Recent computational works on this cluster have given reasonable results for the adsorption energies of several molecules including formaldehyde, formic acid and a series of primary alcohols, when compared to other works [41,42]. As shown in Fig. 5, acrolein is adsorbed via the oxygen of the carbonyl group with minimal perturbation (compare the IR frequencies of adsorbed acrolein to those of the free molecule in Table 2). The adsorption energy is relatively weak, ca. 21 kcal/mol, when compared to that of the alcohols or carboxylic acids on this surface [41,42]. For comparison the adsorption energy of CH_2=$CHCH_3$ was also computed and was found to be unbound by 0.5 kcal/mol, indicating the very weak nature of adsorption of the olefin group on the surface of TiO_2.

4.2. Reductive coupling

Fig. 1 and Table 1 show the formation of C_6 olefins and benzene from acrolein on the reduced surface of

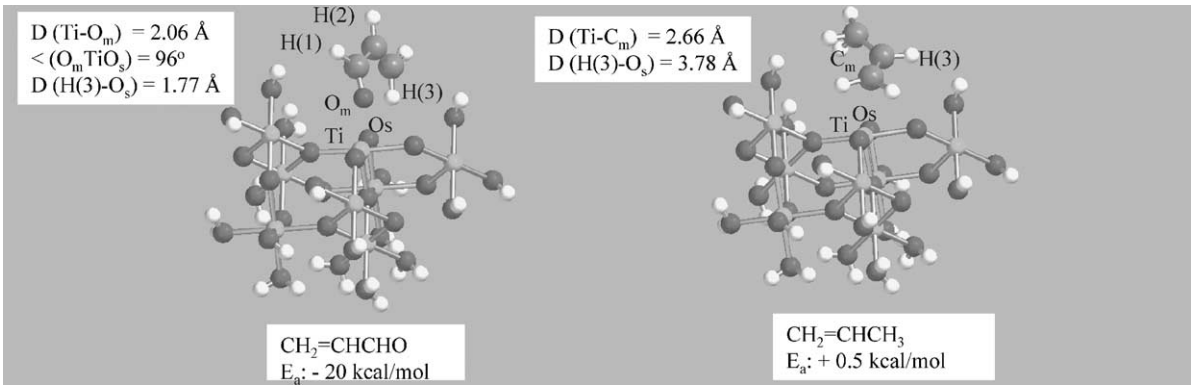

Fig. 5. Acrolein molecule on a $Ti_8O_{29}H_{26}$ charge neutral cluster representing TiO_2(0 1 1) surface. IR frequencies of the free and adsorbed acrolein molecules are also given in Table 2.

a TiO_2(0 0 1) single crystal. The formation of olefins from carbonyl-containing molecules has been observed previously on this same surface. Acetaldehyde [10], acetone [25], *p*-benzoquinone [23], acetophenone [20], and benzaldehyde [24] were all found to undergo reductive coupling. The formation of C_6 products during the reactions of CH_2=CH–CHO can be described by reactions (1)–(3). Here, V_o represents a lattice oxygen vacancy, while O_s represents a lattice oxygen anion

$$2CH_2{=}CH{-}CHO + 2V_o \rightarrow CH_2{=}CH{-}CH{=}CH{-}CH{=}CH_2 + 2O_s \text{ (Reductive coupling)} \quad (1)$$

$$CH_2{=}CH{-}CH{=}CH{-}CH{=}CH_2 \rightarrow C_6H_6 + 2H_{(a)} \text{ (Dehydrocyclization)} \quad (2)$$

$$CH_2{=}CH{-}CH{=}CH{-}CH{=}CH_2 + 2H_{(a)} \rightarrow \text{hexadiene(s) (Reduction)} \quad (3)$$

4.3. Condensation reactions on the stoichiometric surface

As shown in Table 1 and Fig. 2, desorption of a product having a molecular weight of 96 was observed for the reaction of acrolein on the stoichiometric surface. This product is the result of a condensation reaction. The stoichiometric surface of TiO_2 showed very high activity for condensation of acetaldehyde to crotonaldehyde and crotyl alcohol in past experiments [44]. However, while acetaldehyde contains hydrogen atoms on the α-carbon, acrolein does not. Thus, while aldol condensation is facile for acetaldehyde, acrolein gives rise to a much lower yield for the condensation

Table 2
Computed IR frequencies for free acrolein molecules and for an adsorbed acrolein on a cluster representing the TiO_2(0 1 1) surface

Mode	Gas phase, experimental (cm^{-1})[a]	Gas phase, H.F. (cm^{-1})[b]	Gas phase, PM3 (cm^{-1})[b]	Adsorbed, PM3 (cm^{-1})[b]
CH_2-ν_a	3103	3404	3142	3123
CH(2)-ν	3028	3371	3051	3062
CH_2-ν	3000	3315		
CH(1)-ν	2800	3155	2925	
C=O-ν	1724	1916	1978	1893
C=C-ν	1625	1837	1848	1787
CH(1)-ip bend	1360	1542	1340	1326
CH(2)-ip bend	1275	1435	1204	
CH_2 rock	912	998	928	976

[a] From NIST (http://www.webbook.nist.gov).
[b] Calculated.

product. The requirement for the condensation of aliphatic aldehydes and ketones on stoichiometric TiO_2 surfaces is essentially the presence of a basic site: lattice oxygen anions. On acidic surfaces such as zeolites, zirconia [49], and alumina [50], aldol condensation can occur by Brønsted acid catalysis, via a different reaction mechanism not discussed here.

Both the base-catalyzed aldol condensation and the related Michael addition are characterized by attack of a nucleophilic carbanion at an sp^2-hybridized carbon of a second molecule. In the case of acrolein on TiO_2 surfaces, the most plausible nucleophile is $CH_3CH^{(-)}CHO$, since the hydrogen atoms on the vinyl ligand are much less acidic than those at the alpha position of aliphatic aldehydes and ketones. Therefore, hydrogen abstraction from the vinyl group of acrolein to form an even more unsaturated species is unlikely. Second, TiO_2 surfaces prepared by sputtering and annealing appear to contain excess hydrogen, as observed in a number of previous reaction studies. Aliphatic aldehydes scavenge this hydrogen to form the corresponding alkoxides (and ultimately the corresponding alcohols). However, a carbanion (needed to initiate condensation) can be formed if a hydride is instead added to a carbon atom in the vinyl group. The preferred position for such addition is readily apparent, as only ($CH_3CH^{(-)}CH{=}O \leftrightarrow CH_3CH{=}CHO^{(-)}$) exhibits resonance stabilization; $^{(-)}CH_2CH_2CHO$ does not. Thus, we propose that the aldol and Michael addition pathways involve nucleophilic attack of $CH_3CH^{(-)}CHO$ on acrolein. The selectivity between aldol condensation and Michael addition is determined by the competition for the nucleophile between the two ends of the α,β-unsaturated carbonyl. Aldol condensation involves an attack at the carbonyl carbon, while for Michael addition the attack is at the terminal end of the vinyl group.

Aldol condensation:

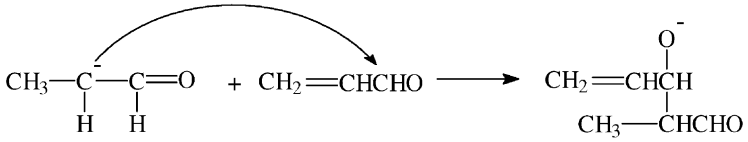

Michael addition:

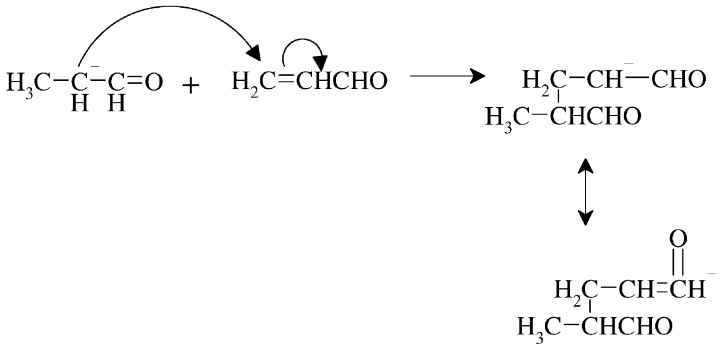

Aldol condensation of acetaldehyde on TiO_2 is accompanied by dehydration to yield crotonaldehyde:

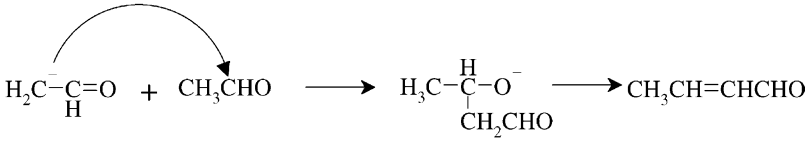

The analogous OH elimination process from the primary acrolein-derived aldol condensation product would produce 2-methyl-2,4-pentadienal:

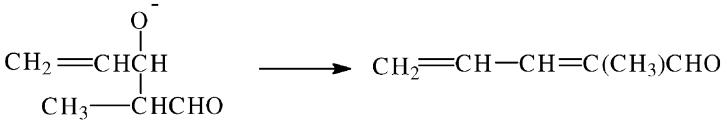

The expected Michael addition product is the result of a net 1,4-hydrogen shift and $H^{(-)}$ elimination:

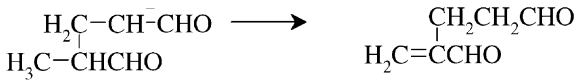

That the latter is not formed as a volatile product from acrolein in our TPD experiments is quite clear; no signal for the corresponding parent ion with $m/e = 112$ was observed. The aldol/dehydration product, 2-methyl-2,4-pentadienal does possess the correct mass (96) and stoichiometry (C_6H_8O) and is the most likely candidate for the 500 K product on stoichiometric surfaces.

The two other potential cyclic isomers, 1-formyl cyclopentene and 2,4-dimethylfuran, would require net 1,4 and 1,5-hydrogen shifts, respectively, in addition to ring closure. While there is ample precedent for cyclization of unsaturated hydrocarbons (e.g. alkynes and allenes on reduced TiO_2(0 0 1) surfaces [46,51]), we have observed little evidence for such chemistry on oxidized surfaces. Likewise, production of formyl cyclopentene from the primary Michael addition product would require a 1,5-hydrogen shift, oxygen elimination and cyclization; production of 1,4-dimethylfuran would require even more rearrangement. It should be noted that while $CH_3CH^{(-)}CHO$ appears to attack acrolein at the expected position for aldol condensation rather than Michael addition, the regioselectivity of H addition to form this nucleophile in the first place is just the opposite. The carbanion required for the subsequent condensation reactions is formed by addition of hydrogen to the terminal methylene group (the point of attack for nucleophiles in Michael addition) rather than at the carbonyl carbon. The carbonyl carbon is the target for aldol condensation, which would likely lead to the formation of allyl alcohol. We have suggested above that the regioselectivity of hydrogen addition to acrolein can be explained in terms of the electron donating characteristics of the vinyl group. Clearly, the structure and size of the attacking nucleophile also play a role: $CH_3CH^{(-)}CHO$ addition appears to occur at the opposite end of the acrolein molecule from the position of initial H addition. Questions about the regioselectivity of nucleophilic reactions on well-defined surfaces have not been widely addressed; further study is clearly needed to provide mechanistic detail for these processes.

Fig. 6 shows results from the full set of experiments to summarize the work in a more quantitative way. The effect of the degree of reduction is well seen on the reductive coupling (as was the case of benzaldehyde [10] and acetaldehyde [24]). Also shown is the condensation product profile that is clearly more pronounced on the stoichiometric surfaces.

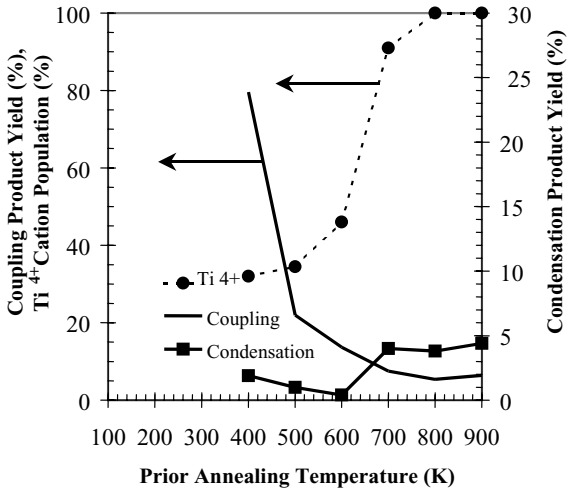

Fig. 6. Change of the population of Ti^{4+} (as determined from the peak area of XPS Ti $2p_{3/2}$), of the condensation product (*m/e* 96 attributed to 2,4-hexadienal), and of the reductive coupling products, all as a function of prior annealing temperatures of TiO_2(0 0 1) single crystal. The yields of both coupling products as a function of prior annealing temperatures are determined as in Table 1. For example, that at 400 K, is that of the Ar^+-sputtered surface that has been annealed to 400 K, and is equal to (hexadiene + hexatriene) = (49.8 + 30.3 = 80.1).

5. Conclusions

Two different reaction pathways were observed for acrolein on TiO_2(0 0 1) surfaces, each leading to the formation of C_6 products. The first is the reductive coupling of adsorbed acrolein to form conjugated olefins. This reaction, which involves carbon–oxygen bond dissociation and carbon–carbon bond formation, was observed mainly on reduced surfaces of TiO_2(0 0 1). The second reaction pathway involving the production of the condensation product C_6H_8O, assigned as 2-methyl-2,4-pentadienal, was more pronounced on the stoichiometric surface. However, the absence of hydrogen in the α-position of acrolein limited this pathway to low product yield. NEXAFS spectra collected from both reduced and stoichiometric TiO_2(0 0 1) surfaces suggested two different adsorbed states. The adsorbates on the reduced TiO_2(0 0 1) surface potentially represent a spectroscopic glimpse of the pinacolate intermediate proposed for the coupling reaction. A more general scheme relating coupling (condensation) reactions of acrolein to the extent of reduction (oxidation) of the surface is presented.

References

[1] M.T. Sananes, G.J. Hutchings, J.-C. Volta, Chem. Commun. (1995) 243.
[2] P.L. Gai, K. Kourtakis, Science 267 (1995) 661.
[3] US Patent 4,767,739 (1988).
[4] J.G. Nunan, C.E. Bogdan, C.E. Klier, K.J. Smith, C.-W. Yong, R.G. Herman, J. Catal. 113 (1988) 410.
[5] A. Deluzarche, J.-P. Hindermann, A. Kiennemann, R. Kieffer, J. Mol. Catal. 31 (1985) 225.
[6] A. Kiennemann, H. Idriss, R. Kieffer, P. Chaumette, D. Durand, I & EC Res. 30 (1991) 1130.
[7] P. Forzatti, E. Troconi, I. Pasquon, Catal. Rev. Sci. Eng. 33 (1991) 109.
[8] K.S. Kim, M.A. Barteau, J. Catal. 125 (1990) 353.
[9] H. Idriss, K.S. Kim, M.A. Barteau, in: R.K. Grasselli, A.W. Sleight
(Eds.), Structure–Activity and Selectivity Relationships in Heterogeneous Catalysis, Elsevier, Amsterdam, 1991, 327 pp.
[10] H. Idriss, M.A. Barteau, Catal. Lett. 40 (1996) 147.
[11] US Patent 4,316,990 (1982).
[12] T. Kawai, T. Sakata, Chem. Phys. Lett. 72 (1980) 87.
[13] K. Sayama, H. Arakawa, Chem. Lett. 253 (1992) 253.
[14] C.T.K. Thaminimulla, T. Takata, M. Hara, J.N. Kondo, K. Domen, J. Catal. 196 (2000) 362.
[15] H. Idriss, A. Miller, E.G. Seebauer, Catal. Today 33 (1997) 215.
[16] A. Linsebigler, C. Rusu, J.J.T. Yates, J. Am. Chem. Soc. 118 (1996) 5284.
[17] A.L. Linsebigler, G. Lu, J.J.T. Yates, Chem. Rev. 95 (1995) 735.
[18] J. Peral, D.F. Ollis, J. Catal. 136 (1992) 554.
[19] J.E. Rekoske, M.A. Barteau, I & EC Res. 34 (1995) 2931.
[20] H. Idriss, M.A. Barteau, in: M. Guisnet, J. Barbier, J. Barrault, C. Bouchoule, D. Duprez, G. Perot, C. Montassier (Eds.), Heterogeneous Catalysis and Fine Chemicals, vol. III, Elsevier, Amsterdam, 1993, p. 463.
[21] H. Idriss, K.G. Pierce, M.A. Barteau, J. Am. Chem. Soc. 113 (1991) 715.
[22] H. Idriss, M. Libby, M.A. Barteau, Catal. Lett. 15 (1992) 13.
[23] H. Idriss, M.A. Barteau, Langmuir 10 (1994) 3693.
[24] H. Idriss, K.G. Pierce, M.A. Barteau, J. Am. Chem. Soc. 116 (1994) 3063.
[25] K.G. Pierce, M.A. Barteau, J. Org. Chem. 60 (1995) 3063.
[26] J.E. Rekoske, M.A. Barteau, Langmuir 15 (1999) 2061.
[27] R.O.C. Norman, J.M. Coxon, Principles of Organic Synthesis, Chapman & Hall, London (1993).
[28] G. Optiz, I. Loshmann, Angew. Chem. 72 (1960) 523.
[29] H.J. Vebel, K.K. Moll, M. Muehlstedt, J. Prakt. Chem. 312 (1971) 849.
[30] D.J. Titheridge, M.A. Barteau, H. Idriss, Langmuir 7 (2001) 2120.
[31] C.W. Smith, Acrolein, Wiley, New York, 1962.
[32] J.M. Vohs, M.A. Barteau, Langmuir 5 (1989).
[33] H. Idriss, J.P. Hindermann, R. Kieffer, A. Kiennemann, A. Valet, C. Chauvin, J.C. Lavalley, P. Chaumette, J. Mol. Catal. 42 (1987) 405.
[34] H. Idriss, C. Diagne, J.P. Hindermann, A. Kiennemann, M.A. Barteau, J. Catal. 155 (1995) 219.
[35] H. Idriss, M.A. Barteau, Catal. Lett. 26 (1994) 123.
[36] H. Idriss, V.S. Lusvardi, M.A. Barteau, Surf. Sci. 348 (1996) 39.
[37] V.S. Lusvardi, M.A. Barteau, J.G. Chen, J.J. Eng, B. Fruhberger, A. Teplyakov, Surf. Sci. 397 (1998) 237.
[38] H. Idriss, K.S. Kim, M.A. Barteau, Surf. Sci. 262 (1992) 113.
[39] E.I. Ko, J.B. Benziger, R.J. Madix, J. Catal. 62 (1980) 264.
[40] NIST Chemistry Webbook, 2000.
[41] L. Kieu, P. Boyd, H. Idriss, J. Mol. Catal. A 176 (2001) 117.
[42] L. Kieu, P. Boyd, H. Idriss, J. Mol. Catal. A 188 (2002) 153.
[43] H. Idriss, M.A. Barteau, Adv. Catal. 45 (2000) 261.
[44] H. Idriss, K.S. Kim, M.A. Barteau, J. Catal. 139 (1993) 119.
[45] A.B. Sherrill, M.A. Barteau, J. Mol. Catal. A 184 (2002) 301.
[46] K.G. Pierce, M.A. Barteau, J. Phys. Chem. 98 (1994) 3882.
[47] J.G. Chen, Surf. Sci. Rep. 30 (1997) 1.
[48] A.B. Sherrill, V.S. Lusvardi, J. Eng, Jr., J.G. Chen, M.A. Barteau, Catal. Today 63 (2000) 43.
[49] G. Zhang, H. Hattori, K. Tanabe, Appl. Catal. 36 (1988) 189.
[50] German Patent 2,505,580 (1976).
[51] K.G. Pierce, M.A. Barteau, J. Mol. Catal. 94 (1994) 389.